Modeled underwater sound levels in the Pan-Arctic due to increased shipping: Analysis from 2013 to 2019 ⊘

Kevin D. Heaney; Christopher M. A. Verlinden; Kerri D. Seger ; Jennifer A. Brandon
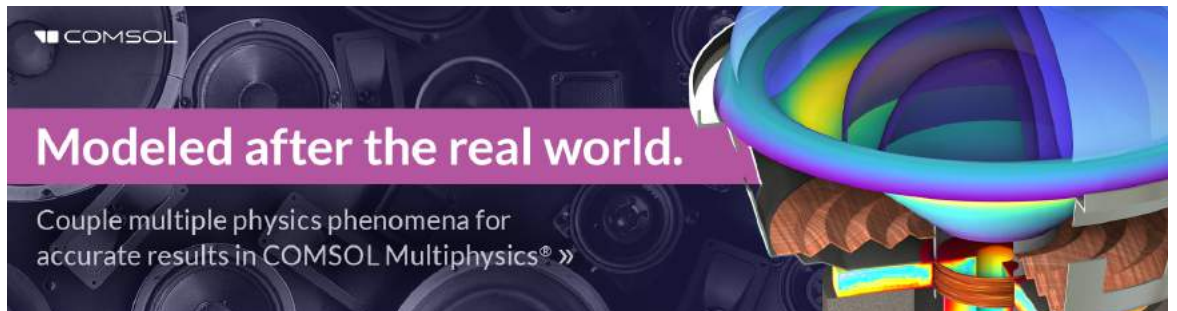
Check for updates

View Online

Export Citation

CrossMark

Modeled underwater sound levels in the Pan-Arctic due to increased shipping: Analysis from 2013 to 2019

Kevin D. Heaney,[a] Christopher M. A. Verlinden, Kerri D. Seger, (iD) and Jennifer A. Brandon

Applied Ocean Sciences, 5242 Port Royal Road #1032, Springfield, Virginia 22151, USA

ABSTRACT:

The loss of Arctic sea ice is one of the most visible signs of global climate change. As Arctic sea ice has retreated, Arctic marine shipping has increased. The Pan-Arctic's unique underwater acoustic properties mean that even small increases in ship traffic can have a significant effect on the ambient soundscape. This study presents the first long-term, basin-scale model of shipping noise in the Pan-Arctic with a focus on a few select sub-regions. The Arctic Ship Traffic Database from the Protection of the Arctic Marine Environment is used in this study to model the locations and source levels from ships operating in the Pan-Arctic between 2013 and 2019. The acoustic footprint of these ships is explored temporally for the entire basin as well as for the select large maritime ecosystems of the Barents Sea, the Northern Bering-Chukchi Sea, and Baffin Bay. From 2013 to 2019, modeled shipping noise propagating underwater broadly increased between 5–20 dB across the Pan-Arctic, but more specific results in sub-regions are presented and discussed. © *2024 Acoustical Society of America.* https://doi.org/10.1121/10.0024354

I. INTRODUCTION

A. SHIPPING IN THE CHANGING ARCTIC

One of the most dramatic effects of global climate change is the reduction in Arctic sea ice. Arctic Ocean warming has been especially significant in recent years compared to the last 100 years. The warming rates of sea surface temperatures are three times the global average; as a result, winter sea ice thickness has reduced by nearly 0.75 m since 1965, declining 11.5% per decade since 1979.[1,2] The annual durations of ice melt and formation seasons have also been changing.[3] Area covered by four-year or older sea ice decreased from 2.7×10^6 km^2 to 53 000 km^2 between September 1984 and September 2019.[4] An ice-free Arctic Ocean during boreal summers is a real possibility by the 2030s,[5] at which time commercial, military, leisure, and fishing vessels could more easily transit through Arctic waters. As the Northwest Passage opens to shipping traffic, the impact from shipping noise on this relatively untouched ecosystem must be monitored and studied.

In the past two decades, boreal summer shipping activity has increased, coinciding with reductions in Arctic sea ice and a shift to predominantly seasonal, instead of year-round, ice cover. A recent assessment of Arctic shipping trends by the Arctic Council Protection of the Arctic Marine Environment (PAME) working group illustrated that the number of ships entering Arctic waters [defined by International Maritime Organization (IMO) Polar Code boundaries] grew by 25% from 2013 to 2019.[6] The total distance these vessels sailed grew by 75%, from 6.1×10^6 nautical miles in 2013 to 10.7×10^6 nautical miles in 2019.[7] Furthermore, the distance bulk carriers sailed in the Arctic Polar Code area increased by 160%. Such an increase in shipping will lead to a louder underwater Pan-Arctic soundscape[6] as ship noise is considered the largest contributor to underwater anthropogenic noise.[8,9]

These percent increases in shipping, while quantified using the IMO Polar Code boundaries that are different than the LME boundaries used in these models, illustrates the general increase in shipping from a Pan-Arctic perspective. In this paper, the long-term (2013–2019) basin and regional-scale acoustic models of the noise generated by shipping across bands relevant to vocalizing Arctic marine mammals are presented. The specific regions of interest include the LMEs of the Barents Sea, the Bering-Chukchi Seas, and Baffin Bay. Sound pressure levels (SPLs) over time from seven distinct spots in these three LMEs will also be presented. From the work of Wenz and Gordon,[10] and the acoustic models that have been developed based on these observations, shipping noise is anticipated to eventually dominate wind noise for frequencies below 300 Hz. The relative ratio of shipping and wind noise to ice noise is a complex subject, and is sensitive to local bathymetry, ice condition, atmospheric forcing, and currents. The observations by Ballard and Sagers[11] and Worcester and Dzieciuch[12] are referred to for long-term observations of the ocean soundscape in the Beaufort.

B. THE ARCTIC OCEAN OCEANOGRAPHY AND SOUNDSCAPE

The soundscapes in and near the Arctic are unique compared to the temperate oceans.[13] Coverage by sea ice prevents the propagation of acoustic waves like those from

[a] Email: OceanSound04@yahoo.com

abiotic, biotic, and anthropogenic sources (e.g., wind, marine mammal, and oil exploration or ship sources, respectively). The presence of ice also reduces contributions from these sources in general by acting like a barrier: preventing wind from creating waves, marine mammals from being in areas with no breathing holes, and/or ships from transiting. For distant sounds, sea ice is not only a scatterer (due to surface roughness), but also an attenuator (*via* conversion to shear waves), so it reduces acoustic propagation when present.[14] This leads to relatively quiet ambient sound levels after ice formation, even though the ice itself generates significant sound during cracking and ridging events. Marine mammal vocalizations are also significant soundscape contributors. Biophonic sources in the areas where models were made largely included signals of residential species, like knocking walruses, singing bowhead whales, whistling and buzzing belugas, and calling ringed seals.[16–18]

Sound propagation is also different in and near Arctic waters compared to temperate regions when ice is not present. Cold air and surface water temperatures in the Arctic create a phenomenon called "surface ducting." This presence of generally upward-refracting sound speed profiles in the Arctic Ocean leads to different acoustic propagation features than in downward-refracting areas of the ocean, even in the absence of ice cover or rough seas.

C. PAN-ARCTIC MARINE SPECIES AND SOUND

The use of underwater sound by Arctic marine animals, including marine mammals, fishes, and invertebrates, is an ongoing area of research. In the oceanic environment, with relatively few anthropogenic sound sources and little light propagation, Arctic marine mammals have evolved to primarily use underwater sound to carry out life functions, such as sensing their environment, navigating, communicating, detecting prey, and avoiding threats like predation.[19] The Arctic is home to 35 marine mammal species for at least part of the year (up to nine are endemic depending on the LME[20]) and it is reasonable to assume that many of these species adapted acoustic communication strategies that are effective both in the presence and absence of sea ice.

Arctic marine mammals are strongly associated with, and can even depend on, sea ice. With climate change, they are particularly vulnerable to habitat loss and to increased competition as more temperate species shift northward, such as fin and humpback whales, which are extending their ranges into the warming Arctic.[6] Industrial development, especially the expansion of shipping, may place additional pressure on these species. Therefore, changing underwater soundscapes as a result of several climate change avenues, plus increased anthropogenic noise, could affect endemic species which have, until recently, had very limited exposure to these noise sources.

This study aimed to determine spatial distribution, levels, and trends of underwater noise from Pan-Arctic shipping between 2013 and 2019. It also makes evident which species' vocalizations these findings would be pertinent for

by focusing on summarizing the frequency ranges used in known repertoires of the endemic and transitory Pan-Arctic marine mammals. To this end, this paper presents the following results:

(1) Modeled shipping-induced underwater noise levels across the Arctic Ocean from 2013 to 2019, including spatial distributions and temporal trends of underwater noise.
(2) An exploration into the implications of underwater noise from shipping for marine mammals, through

    (a) demonstrating overlap in bandwidths produced by shipping and marine mammals, and
    (b) illustrating underwater noise levels in three Pan-Arctic sub-regions with high densities of both ship traffic and marine mammals.

II. METHODS

A. PROCESSING THE ARCTIC SHIPPING TRAFFIC DATASET (ASTD)

The Automatic Identification System (AIS) is a global very high frequency (VHF) radio-based collision avoidance system used by most modern large commercial vessels transiting on international voyages. The system was not originally designed for global monitoring and research, but its data, as collected by ground stations and satellites, can be used to construct vessel tracks for nearly every large commercial vessel at sea at any given time. Along with basic navigational information, including latitude, longitude, course, and speed, AIS also contains information about vessel identity, type, cargo, and size.

AIS data for this analysis came from the Arctic Ship Traffic Data (ASTD)[21] System and was provided by PAME. The data covered January 2013 through April 2020. The entire dataset contained over 1.37×10^9 ship positions and was over 335 GB, with individual months' datasets ranging from 1.5 to 6 GB. The goal of processing this dataset was to construct high-fidelity vessel tracks for the entire Arctic region from 2013 through 2019.

There are two primary identification numbers used to distinguish individual vessels: the Maritime Mobile Service Identity (MMSI) number and the International Maritime Organization (IMO) number. The vast majority of vessel reports contained valid MMSI numbers (99.99%), while fewer reports had associated IMO numbers (62.02%). Many of the reports that had MMSI numbers but not IMO numbers were missing key information, including one or more of vessel class, size, flag state, and status. Reports missing IMO numbers were also more likely to be erroneous by plotting on land or moving faster than physically possible. Any of these errors can result from improperly set up AIS units, poor data governance, or intentional spoofing. Part of the processing required for this analysis was to remove such erroneous and/or incomplete reports.

For the purposes of this analysis, vessel traffic statistics, such as the number of unique vessel MMSI and IMO numbers (Fig. 1), were computed for each individual LME. LMEs are large areas of coastal space, spanning $200\,000\,km^2$ or more, that extend from estuaries or river basins to the margins of major currents or to the edges of continental shelves (Fig. 2). Because this project was performed in collaboration with PAME who uses the LME naming convention, LME boundaries were used as the basis for breaking Arctic and sub-Arctic water masses into regional areas for model development and mapping. Basic entity resolution was applied to synthesize unique vessels, some of which had multiple MMSI numbers in the dataset. Vessel tracks were interpolated to 1 hr intervals, and only vessels over 1000 gross tons (GT) were retained for acoustic simulations (Table I). The final, processed dataset contained 9724 unique vessels.[21]

B. FREQUENCY SELECTION

An in-depth review of the literature on Arctic land and sea use by marine mammals, fish, and seabirds was conducted, anchored in the PAME 2013 Arctic Marine Shipping Assessment (AMSA) IIc, which led to defining which marine mammals were in the three sub-regions of interest, either endemically or transitorily. Using that species information, a literature review of the ranges of their vocalizations (except for the inclusion of an audiogram of the polar bear) was undertaken. By visualizing the ranges of frequencies that marine mammals use in sound production, it is easier to communicate to policymakers about which frequencies most used by the most species in a given region are also the most likely to be masked by shipping noise. With biologically important frequency ranges established, the acoustic propagation models of shipping noise made in this study are more easily interpretable for conservation and management decisions.

This in-depth literature review of sound use by residential and transitory Arctic marine mammals found substantial overlap between frequencies produced and sensed by marine mammals and underwater shipping noise (Fig. 3). In particular, Fig. 3 indicates the acoustic frequency bands utilized by marine mammals present in the three LME regions of interest. These marine mammals utilize a broad range of acoustic frequencies, from 5 Hz to > 200 kHz, which overlap with the natural sonic sources of wind and ice, ranging from 5 Hz to 10 kHz. All Balaenidae whale species and nearly half of the Pan-Arctic Odontoceti species vocalize in (and therefore are also assumed to be auditorily sensitive to) bandwidths also dominated by shipping noise.
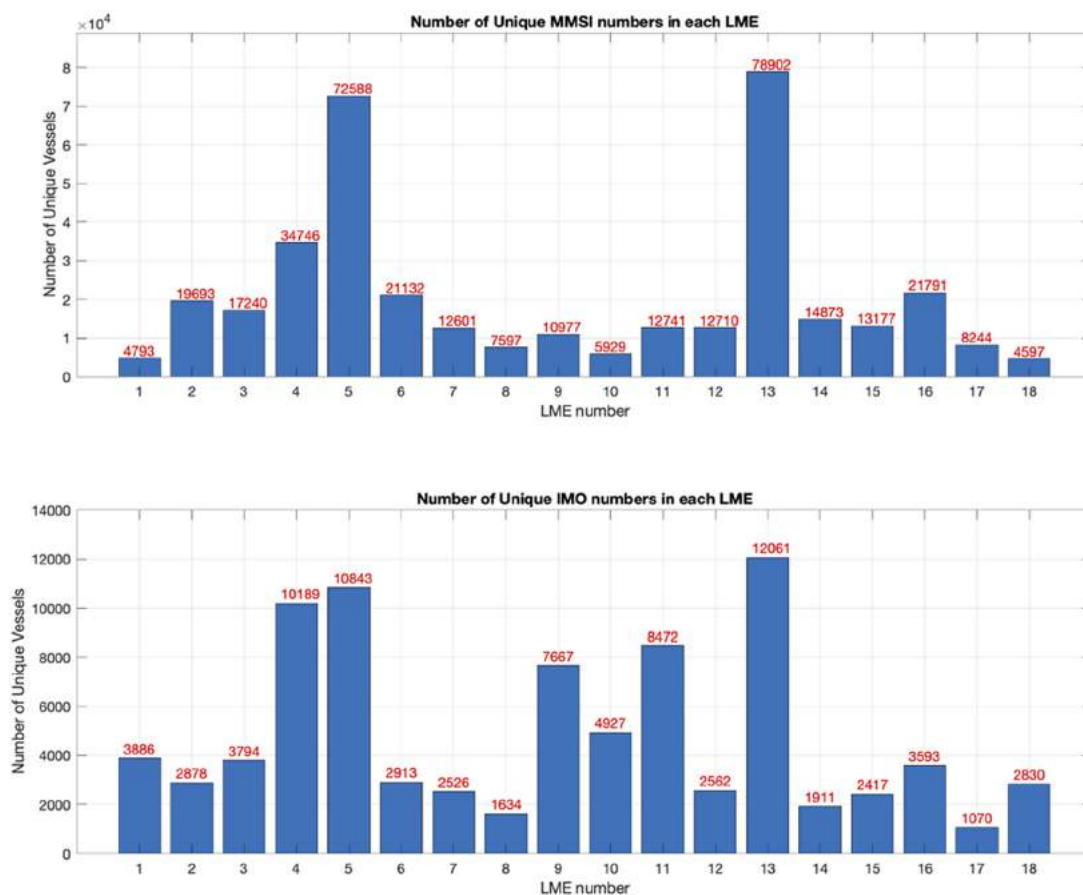

FIG. 1. (Color online) The number of unique Maritime Mobile Service Identity (MMSI) and International Maritime Organization (IMO) numbers by large marine ecosystem (LME) in the raw Arctic Ship Traffic Data (ASTD) Automated Identification System (AIS) dataset. See Fig. 2 for mapped boundaries of each LME number. Reprinted with permission from PAME (2021) (Ref. 23).
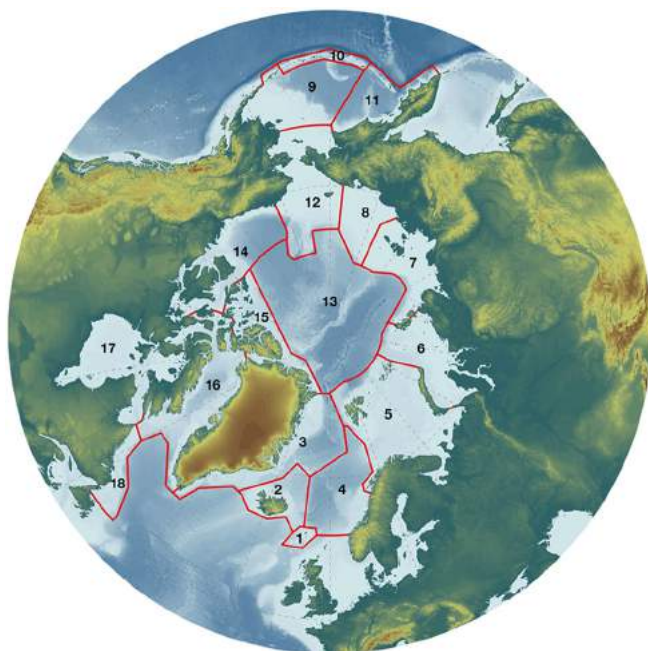
FIG. 2. (Color online) Map of the 18 large marine ecosystems (LMEs) in the Arctic, as adopted by the Arctic Council in May 2013. Reprinted with permission from PAME (2013) (Ref. 22). The Barents Sea LME is five. The Northern Bering-Chukchi Sea LME referred to in this manuscript as the Bering-Chukchi is 12. The Canadian Eastern Arctic-West Greenland LME referred to in this manuscript as Baffin Bay is 16.

To account for the many vocalization frequencies at which marine mammals call, the bandwidth (BW) from 25 Hz to 10 kHz was used in all noise propagation models. Only the lower range results are reported in this manuscript. Shipping source levels tend to peak between 25 and 60 Hz and drop off significantly beyond 500 Hz, but so does average ambient noise due to increased PL at higher frequencies. All acoustic levels reported in this paper are the SPL, which is the modeled received acoustic intensity (pressure-squared) measured in decibels relative to 1 μPa. In the environmental and policy spaces where acoustic soundscapes are used for understanding the environment and the impacts of sound on marine mammals, the reported values of SPL are often given in band-integrated decidecade band levels.[23–25] In this paper, with a deference to the historical use of shipping levels as noise in the sonar equation, the SPL results are presented as spectral levels in dB re 1 μPa^2/Hz. The difference between the two is simply the BW (BW = 0.234 * f_0, where f_0 is the center frequency of the band) of the decidecade band in decibels [$10 \log_{10}$ (BW)].

TABLE I. Requirements for each ship retained in the final analysis. Adapted with permission from PAME (2021) (Ref. 23).

Gross tonnage	>1000 GT
AIS data over 7 years	>100 total points
Gaps between reports	<200 km
MMSI or IMO number	Yes
Hits in 1 month	>60
Speed	1–50 kn

C. SHIPPING SOURCE LEVEL AND PROPAGATION MODELS

The parabolic equation (PE) model was used for the low-frequency (< 1 kHz) propagation modeling. The Bellhop[26] ray trace model was used for propagation modeling of frequency bands over 1 kHz. For the PE model, Heaney and Campbell[27] modified the range dependent acoustic model (RAM), developed by Michael Collins[28] in the 1990s to efficiently handle the full four-dimensional environment. For situations with many ships and time snapshot requirements, the PE model is computationally expensive at high frequencies; thus, it is more suitable for modeling only low-frequency sound.

Environmental inputs required for the acoustic field computation included temperature/salinity, bathymetry, surface conditions (ice and wind), and sediment type. The ocean environment was taken from the Global Hybrid Coordinate Ocean model (HYCOM). Sea-ice extent was taken from the Consortium model for Sea Ice Development[29] (CICE, pronounced "Sea Ice" and not an actual acronym) and hindcasts of the Pan-Arctic Ice-Ocean Modeling and Assimilation System dating back to 2013. It must be noted that the fidelity of oceanographic modeling in the Arctic is severely limited by sparse *in situ* observations and limited surface satellite measurements. Observations of the ocean below the sea-ice cover are limited to a handful of moorings from the ice-tethered program (ITP). An example of this limitation is the inability of HYCOM to produce a sub-surface duct known as the Beaufort Duct, or the Beaufort Lens. This duct is formed by an intrusion of warm Pacific water that leads to a strong sub-surface duct in the southern Beaufort Sea at depths of about 100 m. Improved oceanographic profiles from a 6 year study of the entire Arctic basin were not available for this modeling project.

The bathymetry database used was the General Bathymetric Chart of the Oceans (GEBCO) 2009 dataset and the U.S. Navy Bottom Sediment type (BST) database provided the sediment parameters for the acoustic runs. The BST database categorizes the sediment via a mean grain size. The BST was manually extended north into the Arctic Ocean using water depth as a proxy for grain size. It must be stated that current knowledge of Arctic oceanography, ice morphology, seafloor, and sediment type are severely limited. The model inputs from the environmental databases used for the propagation modeling (bathymetry, sound speed, sediment type, and wind speed) are shown in Fig. 4.

For all model results shown, receiver depths were 10 m below the sea surface. The source depths of all ships were selected from a Gaussian distributed model centered at 6 m with a standard deviation of 1.5 m. Recent models for shipping source level models include Wales and Heitmeyer[31] and the Research Ambient Noise Directionality model (RANDI).[32] After evaluating a significant amount of data, in particular the work by MacGillivray *et al.*,[25] MacGillivray and DeJong[33] determined that speed, vessel length, and class were important additions to the source level model. Their model, which is referred to as the JOMOPANS-ECHO
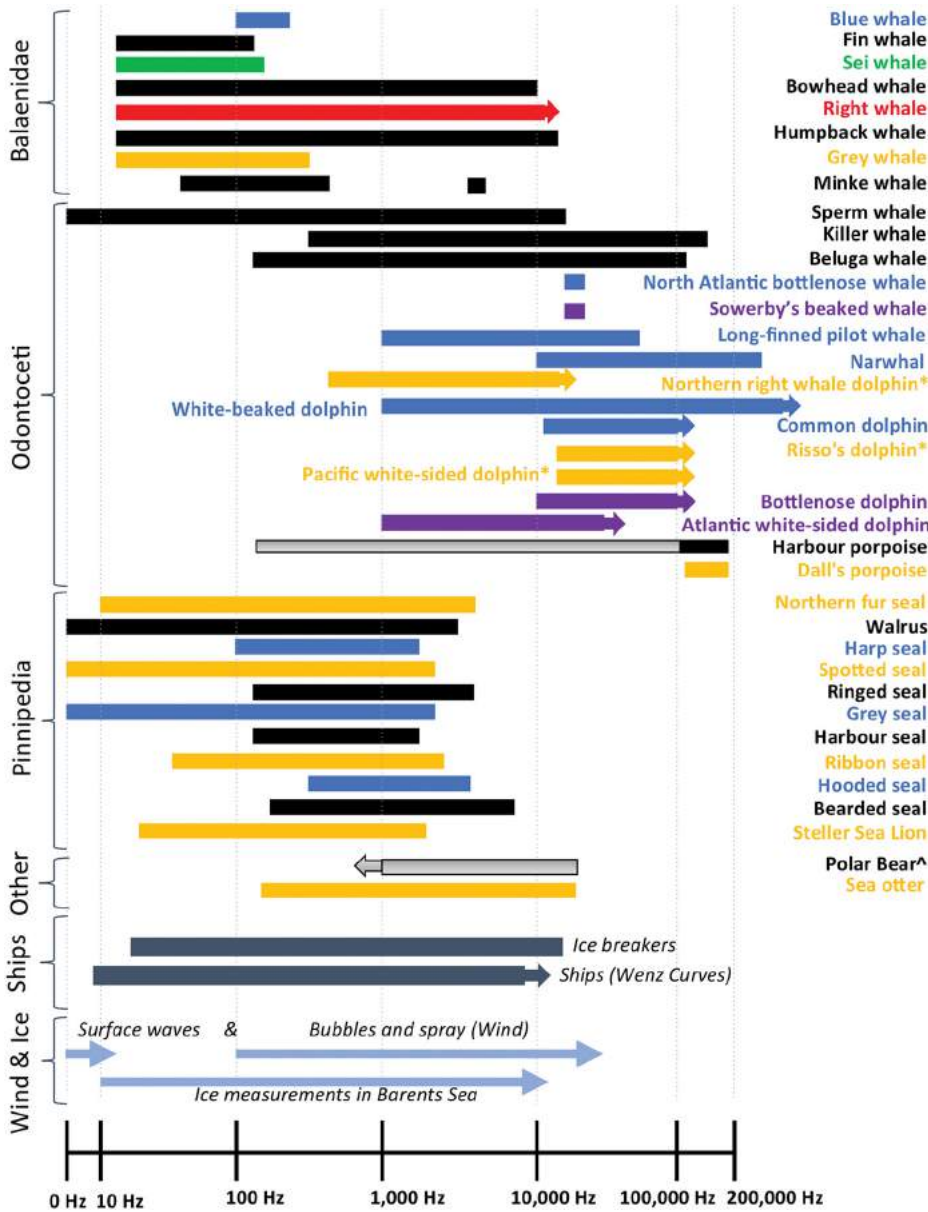
FIG. 3. (Color online) Acoustic overlap between marine mammal vocalizations and other natural and anthropogenic sources in Pan-Arctic soundscapes. Marine mammals are separated into baleen whales (Balaenidae), toothed whales (Odontoceti), seals and sea lions (Pinnipedia), and other [one bear (Ursidae) and one otter (Mustelidae)]. Black bars represent species found in all three regions [Bering-Chukchi (the shortened label for the Northern Bering-Chukchi LME), Barents, Baffin]. Blue bars represent species found in Baffin Bay and Barents Sea. Red bars represent species found in the Bering-Chukchi and Baffin Bay. Orange bars represent species found only in the Bering-Chukchi. Green bars represent species found only in Baffin Bay. Purple bars represent species found only in the Barents Sea. Arrows mean animals could call higher (or lower), but sampling rates of studies done were not high enough to capture the actual highest possible frequency. An asterisk (*) means that the species has either been acoustically or visually documented in that region, but no secondary observations exist to validate the acoustic or visual method, so ranges can be considered extralimital. A review of these species can be found in Seger and Miksis-Olds (Ref. 15). A caret (^) and grayed out arrow means that the audiogram represents sensitivity in air, not in water. Thick navy bars represent ships. Thin blue bars represent ice and wind from the Wenz curves. Reprinted with permission from PAME (2021) (Ref. 23).

model (due to the support of the JOMOPANS[33] and ECHO[25] projects) has the spectral source level (in dB re $\mu Pa^2/Hz$) as

$$[2] \quad \langle L_{S,f}(f) \rangle = 208 - 40 \log_{10}(f_1)$$
$$- 10 \log_{10}\left[\left(1 - \left(\frac{f}{f_1 - 1}\right)^2\right) + D^2\right]$$
$$+ 20 \log_{10}\left[\left(\frac{V}{V_c}\right)^2\left(\frac{l}{l_c}\right)\right],$$

where f is the acoustic frequency in Hertz, $f_1 = 600$ Hz (V_{ref}/V_c), $D = 1$ for vehicle carriers and tankers and 0.8 for container ships and bulkers, V_c is class speed, and l is the ship length, and l_c is class length. The PE model was used to compute propagation loss (PL) of low-frequency bands (<1 kHz) from each ship source's position. Starting with each ship's source level at its particular location in a given

timestamp along its track, a PL field (a.k.a. gridded map) for each ship was calculated in SPL (dB re $\mu Pa^2/Hz$). These modeled PL fields overlapped with each other, and at each point of overlap in the entire gridded map space, the incoherent sum of levels from all ships was calculated. This resulted in a single gridded map for the area of interest of combined SPLs from all ships in each model.

Finally, the number of radials in the models was selected according to the size of the region that was covered. For basin-scale propagation runs, 18 radials were used for the propagation from each ship. Regional models, with smaller spatial scales and where bathymetry effects were expected to be more important, were modeled with 72 radials.

1. Acoustic propagation and sea ice

Several options were available for under-ice propagation including a parabolic equation model which includes shear and a fluid–fluid model using the parabolic equation

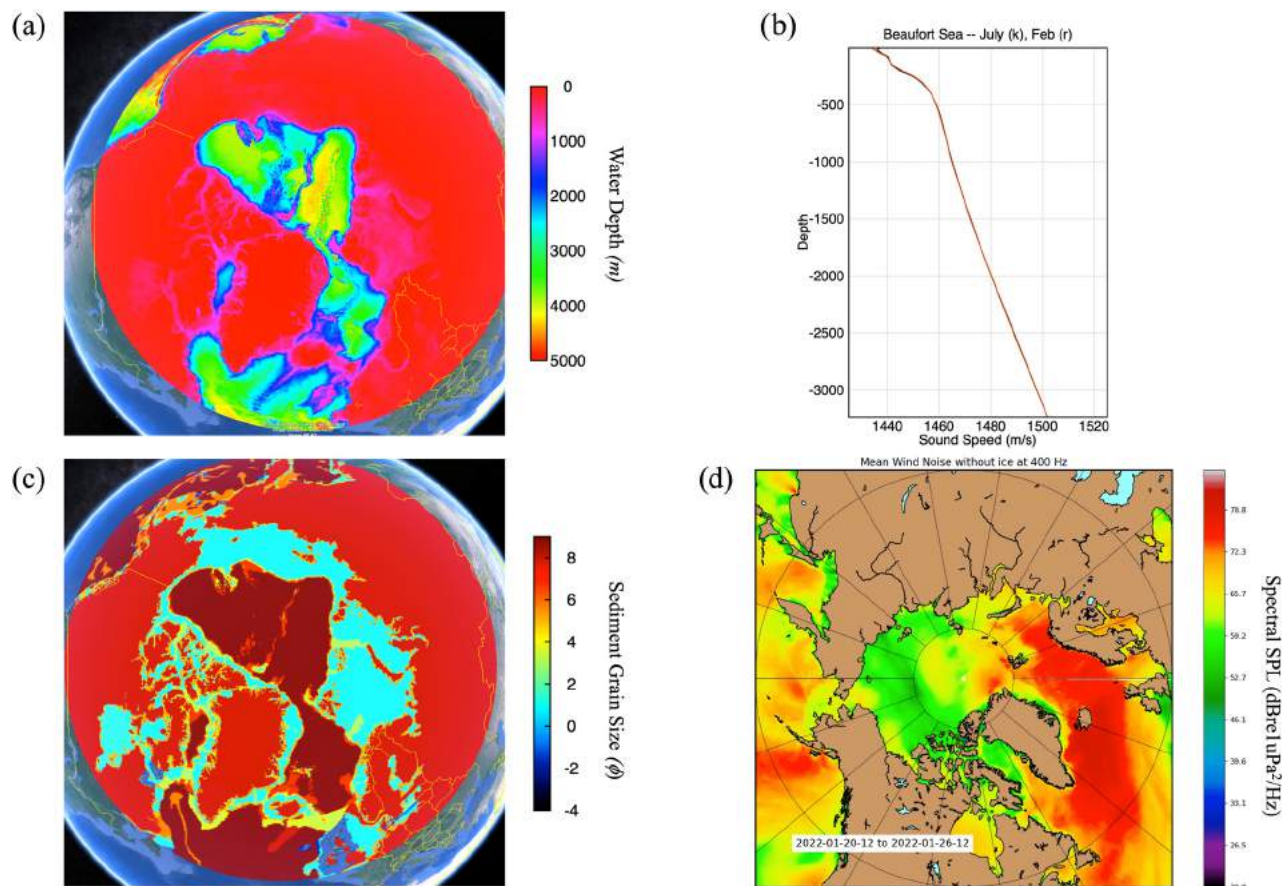J. Acoust. Soc. Am. **155** (1), January 2024

Heaney *et al.*   711

FIG. 4. (Color online) Environmental inputs for the model runs: (a) bathymetry (in meter) from GEBCO 2019 (Ref. 78), (b) sound speed profiles in the Beaufort for July (black) and February (red) from the World Ocean Atlas 2009 (Refs. 79 and 80), (c) bottom sediment grain size parameter (ϕ) extrapolated north from Ref. 81, (d) weekly average of modeled wind noise spectral sound pressure level at 400 Hz for the week of January 20–26, 2022, using the wind noise model developed by F. C. Felizardo, "Ambient noise and surface wave dissipation in the ocean," Ph.D. dissertation (Massachusetts Institute of Technology, 1993) (Ref. 30). Map data reprinted from Google, Data SIO, NOAA, U.S. Navy, NGA, GEBCO Image Landsat/Copernicus Image IBCAO Image U.S. Geological Survey. Copyright 2021.

with a fully range-dependent equivalent ice layer was developed by Heaney and Campbell.[34] In order to increase the speed of computation for the large number of runs required, the complex interaction of sound with the ice canopy was handled via an empirical attenuation as a linear multiplier by the range underneath the ice. To calculate PL at locations where ice was present, the acoustic intensity was attenuated exponentially in range using a dB/km factor taken from the observation work of Buck and Greene[35] (Table II). In summary, only the SPLs were computed, and those levels were primarily dependent upon the total acoustic intensity. In this manner, acoustic fields (PL fields) for both ice-free and ice-present conditions were computed in polar coordinates. Following the addition of ice attenuation to the model calculations, the sound levels were converted from polar to geo-referenced Cartesian coordinates for the computation of the soundscape statistics. Volume attenuation was handled by using Thorp attenuation.

The impact of sea ice on acoustic propagation is illustrated for 250 Hz in Fig. 5. This visualization of the impact of ice on acoustic propagation distinctly shows how, during ice-free boreal summers, a single ship off the west coast of Greenland can ensonify all of Baffin Bay (for 100 s of km), while during ice-covered boreal winters, sound is mostly confined to about only 100 km from the source.

D. STATISTICAL PROCESSING OF ACOUSTIC FIELDS

SPLs vary greatly both temporally and spatially in a soundscape. With acoustic propagation loss, sound levels decrease rapidly with distance from the source (e.g., in spherical spreading conditions, 60 dB are lost over the first

TABLE II. Ice loss vs range values from work by Buck and Greene (Ref. 35).

Frequency (Hz)	Ice loss (dB/km)
25	0.017
63	0.065
125	0.138
250	0.205
1000	0.413
10 000	0.700

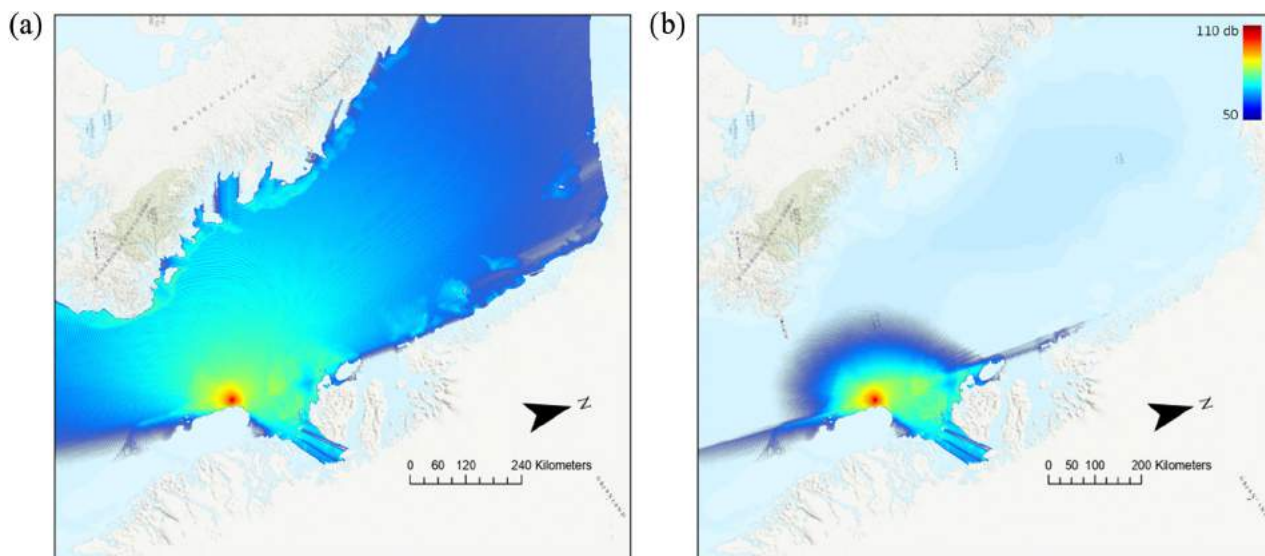712   J. Acoust. Soc. Am. **155** (1), January 2024

Heaney *et al.*

FIG. 5. (Color online) The impacts of sea ice on acoustic propagation at 250 Hz: (a) in an ice-free boreal summer where a single ship off the west coast of Greenland ensonifies the entirety of Baffin Bay, (b) in the boreal winter where the sound is mostly confined to within 100 km of the source. The dynamic range is 50 to 110 dB re 1 μPa^2/Hz. Adapted with permission from PAME (2021) (Ref. 23). Map data reprinted from Google, Data SIO, NOAA, U.S. Navy, NGA, GEBCO Image Landsat/Copernicus Image IBCAO Image U.S. Geological Survey. Copyright 2021.

kilometer). Statistics and associated plots were calculated and made to numerically summarize the visually mapped results of the study. The results of this study showed that the overall sound levels at most geographical points in the study areas were mainly driven by the noise from the closest ship. Areas with few ships had hotspots of localized high sound levels that fluctuated spatially, following the tracks of the ships' routes, and not filling the entire larger study area with high noise levels. In areas with many ships, though, relatively stable sound levels existed across the entire study area. This was less common in the LMEs studied here but would be because many ships in an area would position

them close to each other for most of their transit space, so their noiseprints would overlap and therefore be additive, creating an average, relatively stable sound level across a larger region. Both map figures and statistics calculations dictated capturing these dynamics.

To accurately handle the dynamics of individual ships, 10 min temporal snapshots and 1 km^2 spatial snapshots were required. This resolution was prohibitive for a basin-wide, long-term study, though. To generate accurate and unbiased statistics for a lower-resolution model, PL was spatially averaged first, and then statistics were computed for larger spatial and temporal scales. Individual propagation runs were
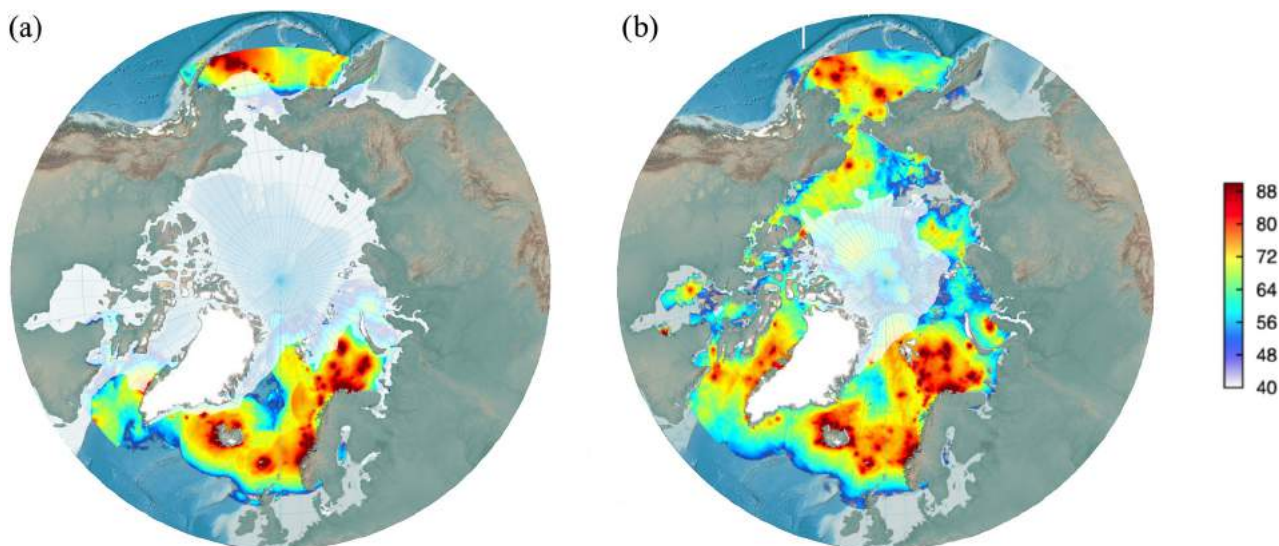

FIG. 6. (Color online) Pan-Arctic 25 Hz weekly median SPL for (a) March 2015, (b) September 2015 (SPL is in units of dB re 1 μPa^2/Hz). Ice extent is shown in translucent white so that sound levels below the ice layer are still visible. Reprinted with permission from PAME (2021) (Ref. 23).
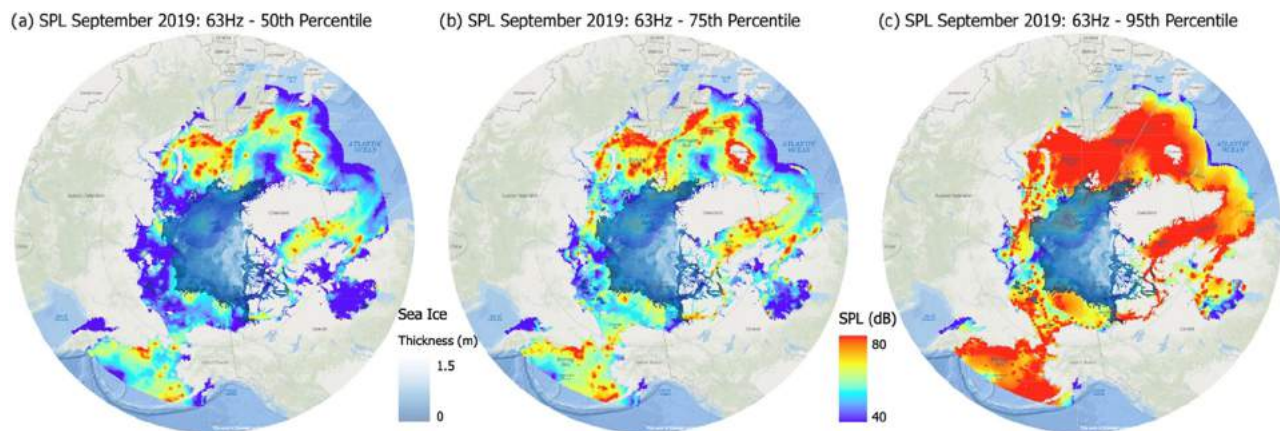
FIG. 7. (Color online) Pan-Arctic 63 Hz weekly average: (a) median, (b) 75th percentile, (c) 95th percentile SPL for July 2015, week 1 (full units for SPL are dB re 1 μPa^2/Hz). Reprinted with permission from PAME (Ref. 23).

computed at 12 h intervals for every ship. The resulting output fields (gridded maps) were generated using 1 km^2 spatial bins. The resulting 1-week averages were from 14 snapshots at 12 h intervals. The spatial bin statistics were generated for 100 km^2 resolution. This smoothing approach is accurate for both regions with many ships and for regions with a single ship. It resulted in distribution characteristics that included both sound level peaks for ship positions and median sound levels in an area that were driven by the number of ships present.

The percentiles (5th, 25th, 50th, 75th, and 95th) of weekly SPLs with a spatial averaging window of 100 km^2 were also calculated. This allowed for comparisons of medians, the maxima void of outliers (95th percentile), and the interquartile distances (75th percentile to 25th percentile) between week, seasons, years, and sub-regions. The maxima and median percentiles are both useful for evaluating ecosystem health and impact on marine fauna.

1. Shipping noise implications for marine mammals

To understand the implications of underwater shipping noise on noise-sensitive species, such as marine mammals, excess noise levels were estimated for each position and time. Excess noise is defined as the amount of noise above an expected background level on a moderately quiet day.[36] The challenge in the Arctic, as compared with the temperate ocean, is the combination of ice cover reducing acoustic propagation distance, noise from the ice itself, and complicated bathymetry. Some measure of the reference natural sound level, therefore, had to be established. An example of a regional measurement in 2019 was done in the Chukchi Sea and collected by Ballard et al.[37] The natural background sound level is expected to vary greatly with location and therefore, the excess noise is not reported in this paper. In the absence of an ice-driven noise model, it should become
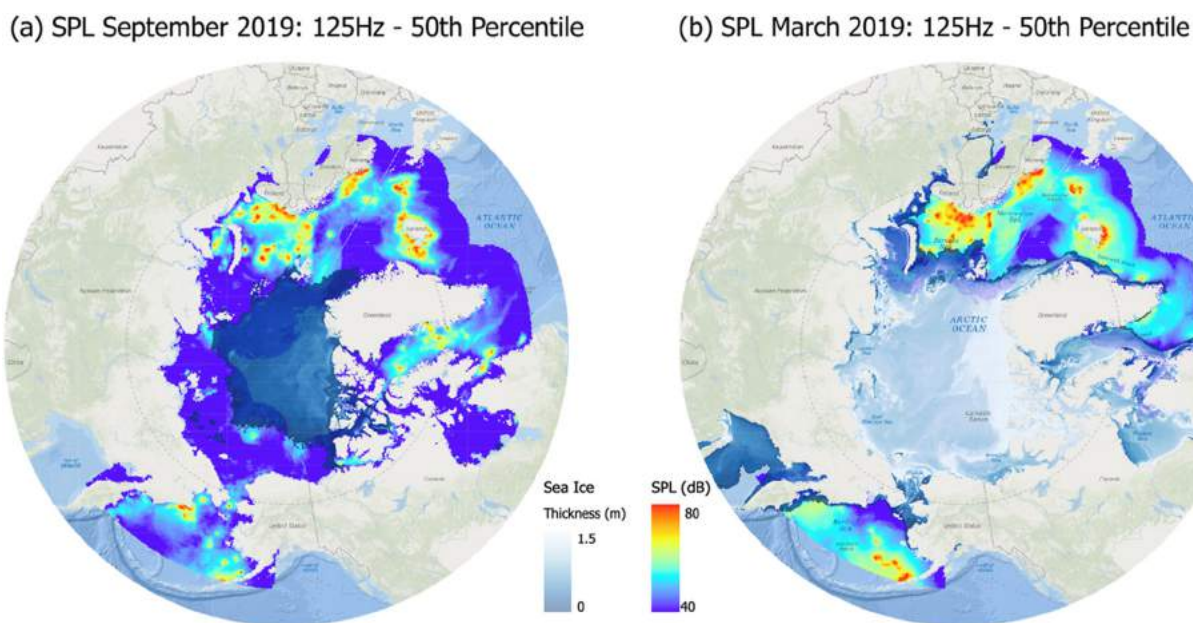
FIG. 8. (Color online) Pan-Arctic 125 Hz band weekly median levels for (a) September 2019, (b) March 2019 (full units for SPL are dB re 1 μPa^2/Hz). Adapted with permission from PAME (2021) (Ref. 23).
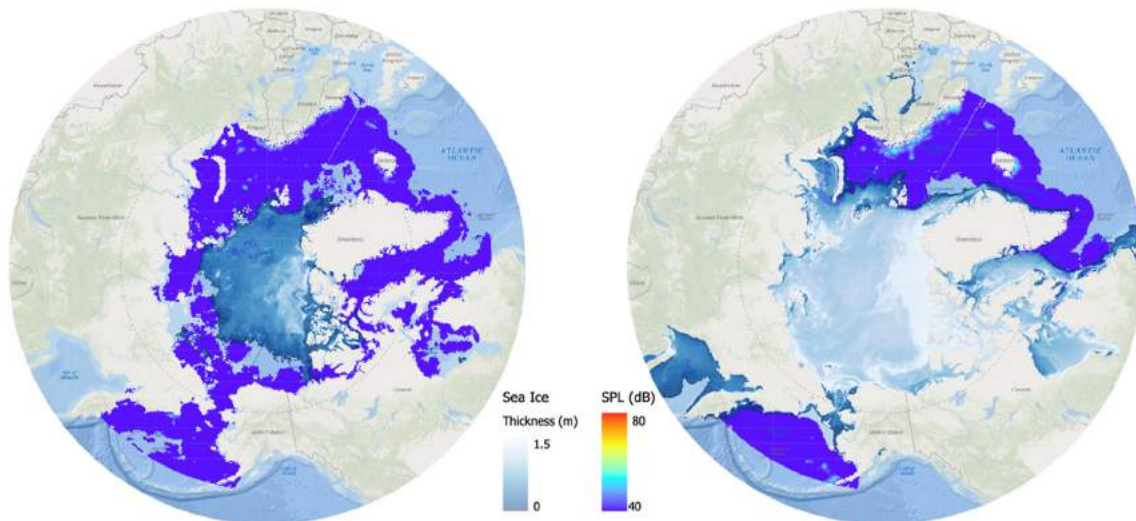
FIG. 9. (Color online) Pan-Arctic 1 kHz weekly median levels for (a) September 2019, (b) March 2019 (SPL is in units of dB re 1 μPa^2/Hz). Adapted with permission from PAME (2021) (Ref. 23).

common practice for natural reference sound levels to be determined by measurement for excess noise studies.

III. RESULTS

A portion of the computed SPLs for the Pan-Arctic region are presented, as well as long-term time series, for the three selected LME sub-regions. The SPLs for the 25 Hz weekly median noise levels for March and September 2015 are shown in Fig. 6. In winter (March), there were high shipping noise levels in the southern Bering Sea, the Barents and Kara Seas, and along the Greenland coast in Baffin Bay [Fig. 6(a), dark red spots]. Note that these weekly median sound levels when ships were present were as intense as 90 dB re 1 μPa^2/Hz. "Average" noise levels in the same areas when ships were not around were only 50 to 70 dB re 1 μPa^2/Hz. In the ice-free boreal summer [September; Fig. 6(b)], shipping noise was distributed more broadly across the Arctic. Sound concentrated in the central Arctic Ocean, the Chukchi and Beaufort Seas, and the Canadian Archipelago. The sound levels in the Beaufort Sea, Barents Sea, and Baffin Bay were substantially higher and propagated further in the summer than in the winter.

Soundscape levels for 63 Hz were higher than at 25 Hz primarily because of the ability of sound waves at 63 Hz to propagate better in shallow, coastal seas. The median SPL for the first week of September 2019 at 63 Hz is shown in Fig. 7(a). During this relatively ice-free period (except the central Arctic Basin), shipping noise was present in all regions, particularly in the Kara Sea (90°E), the Barents Sea (30°E), the Bering and Chukchi Seas (180°E), and in Davis Strait (300°E). The 75th percentile of the 63 Hz SPL for the first week of September 2019 shows high shipping noise levels in the southern Bering Sea, the Barents Sea, and in Baffin Bay [Fig. 7(b)]. In Fig. 7(c), there were regions that experienced 30 dB or more sound levels above their typical medians,

driven by individual ship passes. Here, the underwater contribution of a single ship can clearly be seen in the traffic from the Kara Sea (60°–90°E), the Barents Sea (north of Norway 30°E), the Bering Sea, the Beaufort Sea (180°E), the Davis Strait, and the Canadian Archipelago (270°–330°E). The presence of what was likely a single ship in the central Arctic Basin (60°–90°E, far north) can also be observed. The fact that sounds at a frequency of 63 Hz can travel farther than those at 25 Hz in shallow water is evident in the Kara Sea and the eastern Bering Sea [Fig. 7(b)].
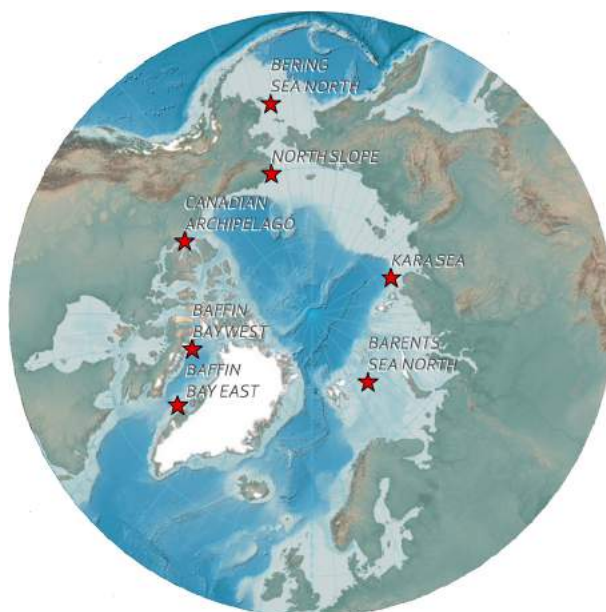

FIG. 10. (Color online) Geographic locations of sites determined to have high levels of both sound and marine mammal activity and so used to calculate modeled spectral SPLs. Reprinted with permission from PAME (2021) (Ref. 23).

The 125 Hz band maps of median shipping SPL (Fig. 8) are shown for 1 week in each March and September 2019. At these frequencies, additional PL from under-ice scattering was significant, and sound propagated relatively short distances. High noise levels occurred again in the Barents Sea, Baffin Bay, and the northern Bering-Chukchi Sea LMEs. Sound waves 125 Hz and higher propagated well in 50–100 m of water, as evidenced in the Bering-Chukchi and Barents Seas.

The 1 kHz SPLs were generated from the Bellhop ray trace model out to a range of 150 km for each ship. These levels are now presented. The 1 kHz band SPL median over a temporal and spatial averaging window of 1 week and
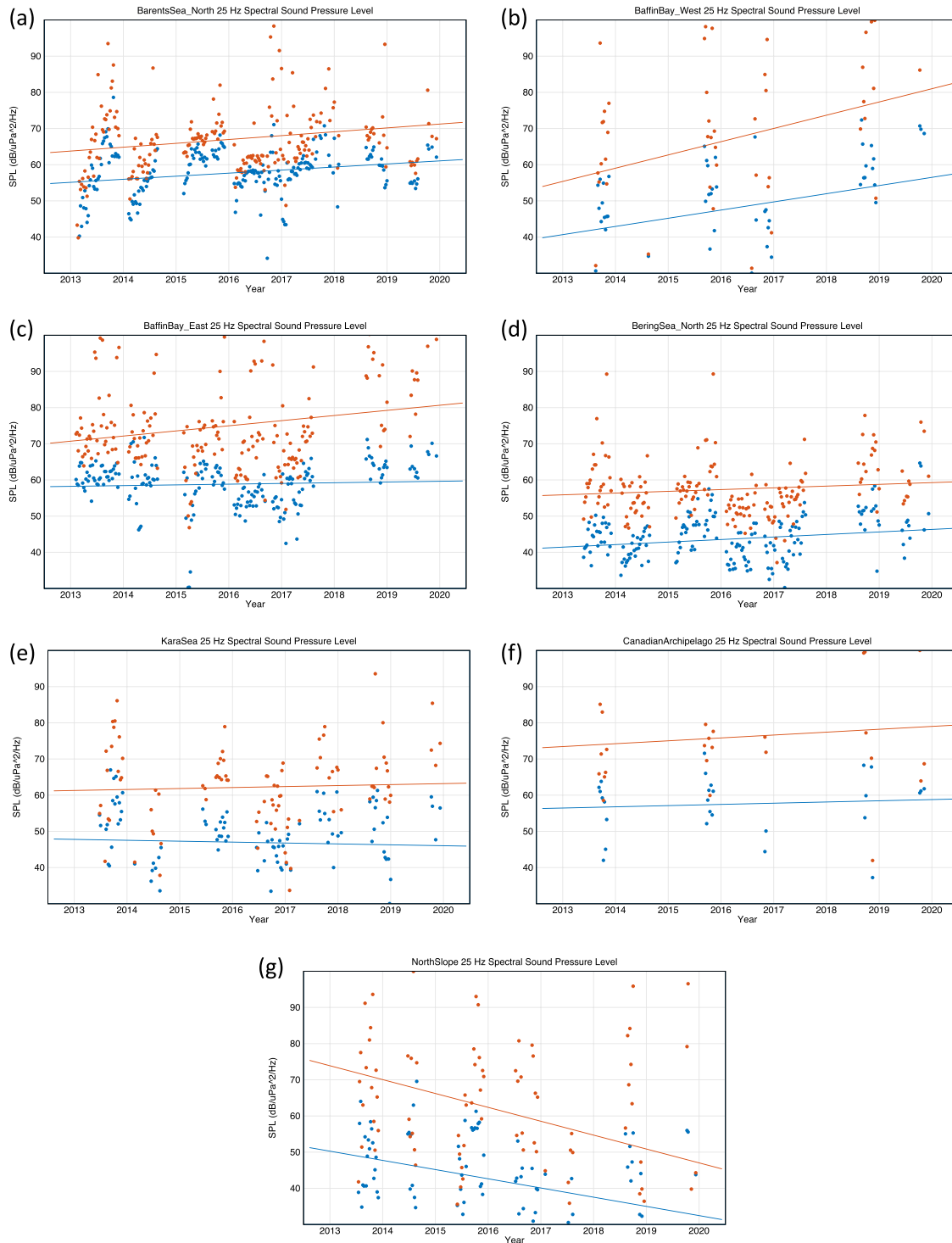

FIG. 11. (Color online) Time series of Pan-Arctic region 25 Hz weekly average median (blue) and 95th (red) percentiles of shipping SPL at the seven selected sites: (a) Northern Barents Sea, (b) Western Baffin Bay, (c) Eastern Baffin Bay, (d) North Bering Sea, (e) Kara Sea, (f) Canadian Archipelago, (g) North Slope. One dot = one weekly average. Trend lines match dot color. There are no dots when there are no ships, likely due to ice cover. (Units of SPL are in dB re 1 μPa^2/Hz). Reprinted with permission from PAME (2021) (Ref. 23).

100 km², respectively, are shown for March and September of 2019 (Fig. 9). The noise levels dropped off quickly when there was only one ship. Singular ships were more apparent in the 1 kHz sound field as compared to the 63 Hz sound field. In the summer, higher sound levels at 1 kHz were observed in the Barents and Bering Seas as compared to in the winter.

1. Temporal trends in underwater noise from Arctic shipping

To evaluate the change in shipping levels between 2013 to 2019, modeled spectral SPLs were extracted at seven locations across the Arctic Ocean (Fig. 10), then plotted as a function of time to investigate intra- and interannual variability (Fig. 11).

The seven specific locations for spectral SPLs within the PAME-defined LMEs were: (1) North Barents (80°N, 40°E), (2) northwestern Baffin Bay (73°N, 74°W), (3) eastern Baffin Bay (68°N, 56°W), (4) the northern Bering Sea (61°N, 169°W), (5) the North Slope (70°N, 165°W), (6) the Kara Sea (78°N,115°E), and (7) the Canadian Archipelago (70°N, 120°W). These areas are distributed across the Pan-Arctic and have been identified as sensitive habitats for marine mammals. The North Barents location lies at the intersection of marine mammal feeding and wintering grounds, having two important haul-out zones for pinnipeds. It is also where blue and fin whales have been documented in the Ocean Biodiversity Information System Spatial Ecological Analysis of Megavertebrate Populations (OBIS) Seamap database[38] and is part of the feeding ground for the Cape Verde and the West Indies humpback whale distinct population segments (DPSs).[39] The northwestern Baffin Bay location lies along the shelf break of Baffin Bay where both killer whales and seals have been commonly documented (OBIS Seamap).[38] The eastern Baffin Bay location is also part of the feeding ground for the West Indies humpback whale DPS. The northern Bering Sea location lies in an important wintering ground for several marine mammal species. Bowhead whales and fin whales frequent this area,[38] and it is just east of an acoustic mooring that documented

habitat expansion for three typically temperate species–Risso's dolphins, Northern right-whale dolphins, and Pacific white-sided dolphins.[16] The Kara Sea location contains islands where beluga whales have been documented in OBIS Seamap[38] and is likely one of their feeding grounds. The Canadian Archipelago location lies at an eastern extreme of the Beaufort Sea where ringed, ribbon, and bearded seals, and beluga and (particularly important for indigenous communities) bowhead whales frequent.[38]

The time series of the weekly median (blue) and 95th percentile (red) measurements and their trend lines for all sites were plotted (Fig. 11). The eastern portion of Baffin Bay [Fig. 11(c)] yielded almost no increase in the median and a small increase in 5–10 dB SPL in the 95th percentile for 25 Hz band noise levels from 2013 to 2019. This increase in the 95th percentile was limited to the summer and is associated with bulk carriers for the Mary River Mine. This eastern region of Baffin Bay has regular heavy shipping due to servicing of the mines along the western coast of Greenland. The western portion of Baffin Bay that has a coastline with eastern Canada [Fig. 11(b)] yielded increases of 15 and 25 dB SPL in the median and 95th percentile levels, respectively. This region is ice-covered for much of the year and, as a result, is usually very quiet.

The northern Barents Sea [Fig. 11(a)] showed a seasonal cycle in its noise signature. Its median SPLs ranged annually from 40 to 70 dB re 1 μPa^2/Hz, but there was no strong increase in median levels over the 7 years calculated. The same general conclusions for the Kara and Laptev Seas [Fig. 11(e)] can be made. In these regions, ship numbers are currently quite small (1–4). Conversely, the sound levels for the North Slope decreased strongly over the 7 years [Fig. 11(g)]. This is most likely due to the withdrawal of Shell Oil in 2014, reducing the noise associated with oil exploration. The same computations were performed for the 63 Hz band and are summarized in Table III.

A high spatial resolution model was run for Baffin Bay and Davis Strait for September 2019. Davis Strait and Baffin Bay were ice-free in September. SPL levels for the 75th percentile were well above 80 dB re 1 μPa^2/Hz in some areas including Disko Bay, Greenland, and in the narrowest

TABLE III. Median and slope vs site (dB re 1 μPa^2/Hz).

Site	Frequency (Hz)	Mean 50th percentile	Mean 95th percentile	Median increase	Peak increase
Baffin Bay West	25	57.8	77.7	13.4	22.7
	63	59.2	78.8	15.6	33.4
Barents Sea North	25	55.4	65.2	6.8	8.5
	63	53.7	75.4	10.3	11.8
Bering Sea North	25	51.4	63.2	5.8	4.2
	63	53.7	67.8	12.4	13.9
Canadian Archipelago	25	64.9	83.2	2.7	6.4
	63	65.7	85.9	2.8	16.4
Kara Sea	25	55.4	71.2	−1.3	3.1
	63	57.3	72.4	8.7	9.1
North Slope	25	51.8	72.3	−15.2	−23.4
	63	50.7	75.4	0.8	2.1

J. Acoust. Soc. Am. **155** (1), January 2024

Heaney *et al.* 717

September 2019 75th Percentile 25 Hz Sound Pressure Level
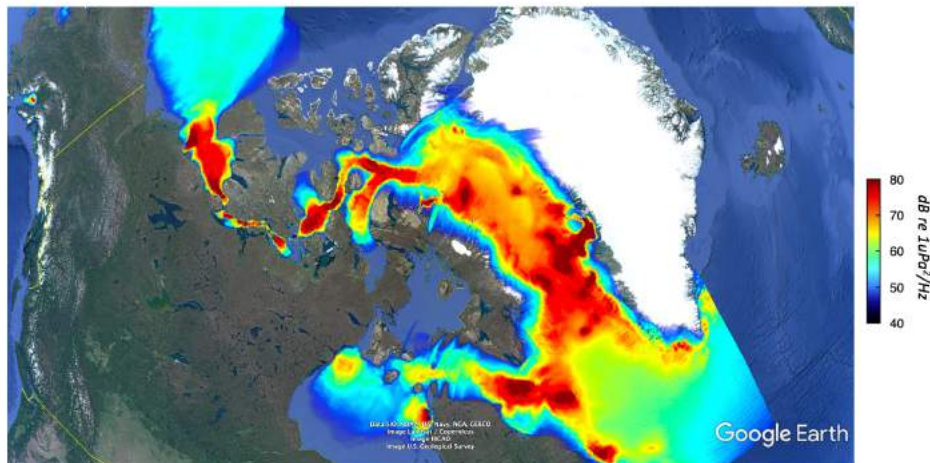
FIG. 12. (Color online) Davis Strait 25 Hz weekly 75th percentile SPL for September 2019, week 1. Units of SPL are in dB re 1 μPa^2/Hz. Adapted with permission from PAME (2021) (Ref. 23). Map data reprinted from Google, Data SIO, NOAA, U.S. Navy, NGA, GEBCO Image Landsat/Copernicus Image IBCAO Image U.S. Geological Survey. Copyright 2021.

part of Davis Strait. A hotspot of sound at the mouth of Hudson Strait, offshore of Killiniq Island, Nunavut, Canada was an obvious acoustic feature in the model (Fig. 12).

Finally, the 95th percentile for the 63 Hz SPL for the first week of September 2019 (Fig. 13) showed high SPLs of low-frequency sound across the Barents Sea, especially along the northwesternmost coast of Russia and the coast of Norway. The primary driver for these hotspots was shipping lanes.

IV. CONCLUSION AND REMARKS

The Arctic Ocean is a unique oceanic acoustic environment with extensive ice cover that both limits the presence of anthropogenic sources and attenuates sound, preventing it from propagating long distances. This polar winter soundscape is dominated by ice noise, wind noise, and marine mammal vocalizations. As the ice retreats, parts of the Pan-Arctic (like western Baffin Bay) become upward-refracting sound speed profiles and the models presented here illustrate how this affects the reach of ship noise throughout three LME sub-regions. The presence of only a few ships in ice-free polar waters can have a large impact on the overall sound levels in the environment. The potential for a completely ice-free boreal summer in approximately a decade means there will be more months of open water in the Pan-Arctic where marine mammals may have to adapt to a louder new normal.

In this study, shipping noise from 2013 through 2019 in the Pan-Arctic basin and several sub-regions was modeled, revealing several areas important to marine mammals with anthropogenic acoustic hotspots. The increases in the spatial median sound levels were greater than 10 dB in the western Baffin Bay, the northern Barents Sea, and the northern Bering Sea. This conclusion was consistent with the PAME 2020 Arctic Shipping Status report, which quantified shipping level increases in the same areas. For locations currently with very few ships, the presence of just a few more in the future will likely increase ambient noise levels greatly across entire subregions.

The selection of which acoustic frequencies to model was guided by identifying those that are both used by marine mammal species and produced by ships transiting the Arctic region. Marine mammals, being air-breathing animals, spend much of their time near the surface. Therefore, the excellent acoustic propagation conditions in a near-surface duct in ice-free waters could exacerbate shipping noise's

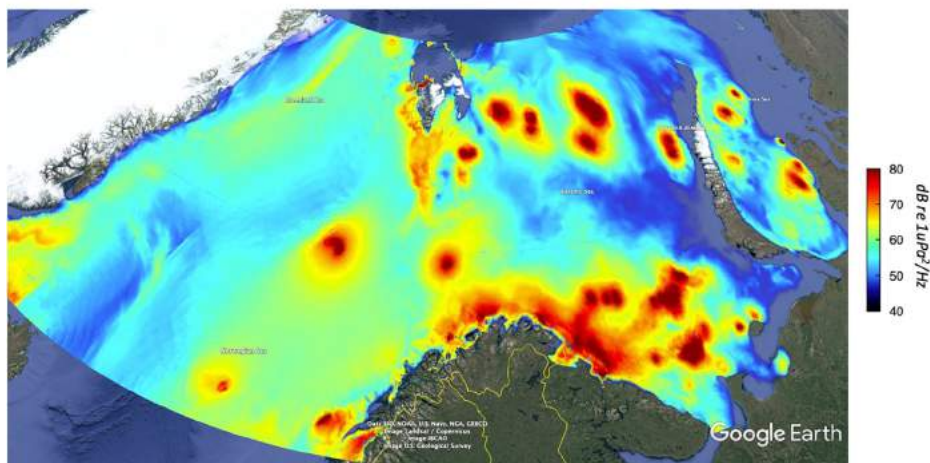September 2019 Median 63 Hz Sound Pressure Level

FIG. 13. (Color online) Barents Sea 63 Hz weekly median sound pressure level for the first week of September 2019. Units of SPL are in dB re 1 μPa^2/Hz. Adapted from PAME (2021) (Ref. 23). Map data reprinted from Google, Data SIO, NOAA, U.S. Navy, NGA, GEBCO Image Landsat/Copernicus Image IBCAO Image U.S. Geological Survey. Copyright 2021.

impacts on these marine mammals in the bands where their frequencies overlap.

The Arctic is not a monolithic ocean. There are regions of vast open water, abyssal seafloor depths, large continental shelves, and complex archipelagos. Some regions are especially environmentally and culturally sensitive to the impact of shipping noise, but the few sub-regions explored in this study do not represent the gamut of all possible scenarios in the Arctic Ocean. In the future, high-resolution, site-specific modeling should be conducted in more areas encompassing more of the range of underwater features to evaluate the impact of anthropogenic sound more holistically across the various marine ecosystems.

This study is entirely model-based and is important primarily because there are very few ambient sound measurements in the Arctic. There is a great need to validate these models because of the uncertainty surrounding acoustic propagation in icy environments and in the source levels of both individual and classes of ships. There is also a need for a better understanding of ice-generated noise and its impact on the Arctic marine ecosystem's natural background SPLs.

Reprinted with permission from PAME (2021) (Ref. 23).

APPENDIX

Marine mammal	Acoustic frequency	Source
Beluga whale	200 Hz to 20 kHz; echolocation clicks extending upward of 120 kHz	Refs. 40 and 41
Killer whale/orca	<500 Hz to 1500 Hz for pulsed calls and whistles; clicks up to 150 kHz at least	Refs. 42 and 43

(Continued)

Marine mammal	Acoustic frequency	Source
Sperm whale	0–24 kHz	Ref. 44
Bowhead whale	20 Hz to 10 kHz	Ref. 45
Humpback whale	20 Hz to 20 kHz	Refs. 46 and 47
Right whale	20 Hz to >16 kHz	Ref. 48
Fin whale	20 Hz to 131 Hz	Ref. 49
Minke whale	5–6 kHz clicks	Refs. 50–52
	80–118 Hz downsweeps	
	58–500 Hz	
Blue whale	100–300 Hz	Ref. 49
Sei whale	21–100 Hz	Refs. 53–55
	35–129 Hz	
Narwhal	clicks 10–240 kHz	Ref. 56
Grey whale	20 Hz to 2 kHz	Refs. 57–59
	45 Hz to 4.520 kHz	
Risso's dolphin	20 Hz to about 100 kHz	Ref. 60
Northern right whale dolphin	6 kHz to >22 kHz	Ref. 53
Pacific white-sided dolphin	20 kHz to about 100 kHz	Ref. 60
North Atlantic bottle-nose whale*	31–39 kHz	Ref. 49
Sowerby's beaked whale*	31–39 kHz	Ref. 49
Long-finned pilot whale	1–15 kHz	Refs. 61 and 62
	2.5–75 kHz	
White-beaked dolphin	Whistles 3–35 kHz	Ref. 63
	clicks 1 kHz to >300 kHz	
Common dolphin	15 kHz to >100 kHz	Ref. 60
Bottlenose dolphin	10 kHz to about 100 kHz	Ref. 60
Atlantic white-sided dolphin	1 kHz to >48 kHz	Ref. 64
Harbour porpoise	110–180 kHz	Ref. 65
Dall's porpoise	130–180 kHz	Ref. 66
Walrus	0–5 kHz	Ref. 67
Steller sea lion	30 Hz to 3 kHz (females)	Ref. 68
Harp seal	100–2500 Hz	Ref. 69
Bearded seal	1–8 kHz	Ref. 49
	300–2500 Hz	Ref. 70
Ribbon seal	50–4000 Hz	Ref. 70
Ringed seal	200–1600 Hz	Ref. 70
Harbour seal	200–2000 Hz	Ref. 71
Spotted seal	0–3 kHz	Ref. 72
Hooded seal	0.5–6 kHz	Ref. 73
Grey seal	0–3.5 kHz	Ref. 74
Polar bear	1–30 kHz IN AIR	Ref. 75
Sea Otter	270 Hz to 13 kHz	Ref. 76
Northern Fur Seal	10 Hz to 6 kHz	Ref. 77

[1] J. C. Comiso and D. K. Hall, "Climate trends in the Arctic as observed from space," Wiley Interdiscip. Rev.: Clim. Change **5**(3), 389–409 (2014).

[2] M. Steele, W. Ermold, and J. Zhang, "Arctic Ocean surface warming trends over the past 100 years," Geophys. Res. Lett. **35**(2), L02614, https://doi.org/10.1029/2007GL031651 (2008).

[3] S. E. Howell, C. R. Duguay, and T. Markus, "Sea ice conditions and melt season duration variability within the Canadian Arctic Archipelago: 1979–2008," Geophys. Res. Lett. **36**(10), L10502, https://doi.org/10.1029/2009GL037681 (2009).

[4] "Falling up," available at http://nsidc.org/arcticseaicenews/2019/10/falling-up/ (Last viewed December 1, 2021).

J. Acoust. Soc. Am. **155** (1), January 2024

Heaney *et al.*   719

[5] G. Peng, J. L. Matthews, M. Wang, R. Vose, and L. Sun, "What do global climate models tell us about future Arctic sea ice coverage changes?," Climate **8**(1), 15 (2020).

[6] PAME, "Underwater noise in the Arctic: A state of knowledge report," (2019).

[7] H. Hreinsson, "The increase in arctic shipping 2013-2019: Arctic Shipping Status Report (ASSR) #1," (2020).

[8] M. A. McDonald, J. A. Hildebrand, and S. M. Wiggins, "Increases in deep ocean ambient noise in the Northeast Pacific west of San Nicolas Island, California," J. Acoust. Soc. Am. **120**(2), 711–718 (2006).

[9] R. K. Andrew, B. M. Howe, J. A. Mercer, and M. A. Dzieciuch, "Ocean ambient sound: Comparing the 1960s with the 1990s for a receiver off the California coast," Acoust. Res. Lett. Online **3**(2), 65–70 (2002).

[10] G. M. Wenz, "Acoustic ambient noise in the ocean: Spectra and sources," J. Acoust. Soc. Am. **34**(12), 1936–1956 (1962).

[11] M. S. Ballard and J. D. Sagers, "Clustering analysis of a yearlong record of ambient sound on the Chukchi Shelf in the 40 Hz to 4 kHz frequency range," J. Acoust. Soc. Am. **150**(3), 1597–1608 (2021).

[12] P. F. Worcester and M. Dzieciuch, "The ambient noise environment of the Canada Basin during the year 2016–2017," J. Acoust. Soc. Am. **146**(4), 3026 (2019).

[13] S. M. Haver, H. Klinck, S. L. Nieukirk, H. Matsumoto, R. P. Dziak, and J. L. Miksis-Olds, "The not-so-silent world: Measuring Arctic, Equatorial, and Antarctic soundscapes in the Atlantic Ocean," Deep Sea Res. Part I: Oceanogr. Res. Pap. **122**, 95–104 (2017).

[14] L. M. Brekhovskih, V. V. Goncharov, and V. M. Kurtepov, "Weakly divergent bundles of sound rays in the Arctic," Oceanogr. Lit. Rev. **1**(44), 16 (1997).

[15] K. D. Seger and J. Miksis-Olds, "First acoustic documentation of non-traditional Arctic species in the Bering and Chukchi Seas," Mar. Mamm. Sci. **35**, 1099–1111 (2019).

[16] K. D. Seger and J. L. Miksis-Olds, "A decade of marine mammal acoustical presence and habitat preference in the Bering Sea," Polar Biol. **43**(10), 1549–1569 (2020).

[17] J. L. Miksis-Olds, P. J. Stabeno, J. M. Napp, A. I. Pinchuk, J. A. Nystuen, J. D. Warren, and S. L. Denes, "Ecosystem response to a temporary sea ice retreat in the Bering Sea: Winter 2009," Prog. Oceanogr. **111**, 38–51 (2013).

[18] J. L. Miksis-Olds and L. E. Madden, "Environmental predictors of ice seal presence in the Bering Sea," PLoS One **9**(9), e106998 (2014).

[19] P. L. Tyack, "Implications for marine mammals of large-scale changes in the marine acoustic environment," J. Mammal. **89**(3), 549–558 (2008).

[20] CAFF, "Arctic Biodiversity Assessment. Status and trends in Arctic biodiversity," Conservation of Arctic Flora and Fauna, Akureyri (2013).

[21] H. Hreinsson, "Arctic Shipping Traffic Dataset (ASTD)," Protection of the Marine Environment (PAME), Arctic Council (2018).

[22] PAME, "Large Marine Ecosystems (LMEs) of the Arctic area, Revision of the Arctic LME Map," 2nd ed., Arctic Council (2013).

[23] J. Brandon, K. Heaney, K. Seger, C. Verlinden, M. Schuster, A. Dumbrille, M. Lancaster, T. Munoz, A. Heaney, S. Rosenthal, A. Azzara, D. Fraser, J. Gedamke, L. Hatch, L. Herata, F. Holz, H. Hreinsson, M. Muller, and P. Winsor, "PAME, Underwater Noise POllution From Shipping in the Arctic" (2021).

[24] M. A. Ainslie *et al.*, "Project Dictionary: Terminology Standard. Document 02075," Version 1, Technical Report by JASCO Applied Sciences for ADEON, (2020).

[25] A. O. MacGillivray, Z. Li, D. E. Hannay, K. B. Trounce, and O. M. Robinson, "Slowing deep-sea commercial vessels reduces underwater radiated noise," J. Acoust. Soc. Am. **146**(1), 340–351 (2019).

[26] M. B. Porter, "The bellhop manual and user's guide: Preliminary draft," Technical Report No. 260, Heat, Light, and Sound Research, Inc., La Jolla, CA (2011).

[27] K. D. Heaney and R. L. Campbell, "Three-dimensional parabolic equation modeling of mesoscale eddy deflection," J. Acoust. Soc. Am. **139**(2), 918–926 (2016).

[28] M. D. Collins, "A split-step Padé solution for the parabolic equation method," J. Acoust. Soc. Am. **93**(4), 1736–1742 (1993).

[29] Naval Research Laboratory, "Global Ocean Forecast System (GOFS) 3.1 (2014-2021)," available at https://www7320.nrlssc.navy.mil/dynamic/gofs/gofs.php (Last viewed December 13, 2020).

[30] F. C. Felizardo, "Ambient noise and surface wave dissipation in the ocean," Ph.D. dissertation, Massachusetts Institute of Technology, Cambridge, MA, 1993.

[31] S. C. Wales and R. M. Heitmeyer, "An ensemble source spectra model for merchant ship-radiated noise," J. Acoust. Soc. Am. **111**(3), 1211–1231 (2002).

[32] J. E. Breeding, Jr., M. Bradley, M. H. Walrod, and W. McBride, "Research Ambient Noise DIrectionality (RANDI) 3.1 Physics Description," Naval Research Lab Stennis Space Center MS (1996).

[33] A. MacGillivray and C. de Jong, "A reference spectrum model for estimating source levels of marine shipping based on Automated Identification System data," J. Mar. Sci. **9**(4), 369 (2021).

[34] K. Heaney and R. Campbell, "Effective ice model for under-ice propagation using the fluid-fluid parabolic equation," Proc. Mtgs. Acoust. **19**, 070052 (2013).

[35] B. M. Buck and C. R. Greene, "Arctic deep-water propagation measurements," J. Acoust. Soc. Am. **36**(8), 1526–1533 (1964).

[36] European Environment Agency, "Noise in Europe 2014, EEA Report No. 10/2014." (2014), 62 pp., http://www.eea.europa.eu/publications/noise-in-europe-2014.

[37] M. S. Ballard, M. Badiey, J. D. Sagers, J. A. Colosi, A. Turgut, S. Pecknold, Y.-T. Lin, A. Proshutinsky, R. Krishfield, P. F. Worcester, and M. M. A. Dzieciuch, "Temporal and spatial dependence of a yearlong record of sound propagation from the Canada Basin to the Chukchi Shelf," J. Acoust. Soc. Am. **148**(3), 1663–1680 (2020).

[38] P. N. Halpin, A. J. Read, E. Fujioka, B. D. Best, B. Donnelly, L. J. Hazen, C. Kot, K. Urian, E. LaBrecque, A. Dimatteo, J. Cleary, C. Good, L. B. Crowder, and K. D. Hyrenbach, "OBIS-SEAMAP: The world data center for marine mammal, sea bird, and sea turtle distributions," Oceanog. **22**(2), 104–115 (2009).

[39] NMFS, NOAA, "Endangered and threatened species; identification of 14 distinct population segments of the humpback whale (Megaptera novaeangliae) and revision of species wide listing," Fed Regist. **81**, 62260–62320 (2016), available at https://www.jstor.org/stable/24860963.

[40] W. W. L. Au, Whitlow, D. A. Carder, R. H. Penner, and B. L. Scronce, "Demonstration of adaptation in beluga whale echolocation signals," J. Acoust. Soc. Am. **77**(2), 726–730 (1985).

[41] B. L. Sjare and T. G. Smith. "The relationship between behavioral activity and underwater vocalizations of the white whale, *Delphinapterus leucas*," Can. J. Zool. **64**(12), 2824–2831 (1986).

[42] O. A. Filatova, P. J. O. Miller, H. Yurk, F. I. P. Samarra, E. Hoyt, J. K. B. Ford, C. O. Matkin, and L. G. Barrett-Lennard, "Killer whale call frequency is similar across the oceans, but varies across sympatric ecotypes," J. Acoust. Soc. Am. **138**(1), 251–257 (2015).

[43] J. Wladichuk, S. Dosso, J. Koblitz, and J. Lawson, "Source level measurements of killer whale (Orcinus orca) echolocation clicks," J. Acoust. Soc. Am. **148**(4), 2632–2633 (2020).

[44] J. C. Goold and S. E. Jones. "Time and frequency domain characteristics of sperm whale clicks," J. Acoust. Soc. Am. **98**(3), 1279–1291 (1995).

[45] See the Audio Gallery (DOSITS.org) for spectrograms and recordings of vocalizations of various marine mammal species of interest.

[46] Catalogue of the Humpback Whale Social Call Working Group (managed by Dr. K.D. Seger).

[47] C. E. Perazio and E. Mercado. "Do singing humpback whales (Megaptera novaeangliae) favor specific frequency bands?," J. Acoust. Soc. Am. **144**(3), 1953–1953 (2018).

[48] S. E. Parks, A. Searby, A. Célérier, M. P. Johnson, D. P. Nowacek, and P. L. Tyack, "Sound production behavior of individual North Atlantic right whales: Implications for passive acoustic monitoring," Endangered Species Res. **15**(1), 63–76 (2011).

[49] S. De Vreese, M. van der Schaar, J. Weissenberger, F. Erbs, M. Kosecka, M. Solé, and M. André, "Marine mammal acoustic detections in the Greenland and Barents Sea, 2013–2014 seasons," Sci. Rep. **8**(1), 16882 (2018).

[50] P. Beamish and E. Mitchell, "Short pulse length audio frequency sounds recorded in the presence of a minke whale (*Balaenoptera acutorostrata*)," Deep-Sea Res. Oceanogr. Abstr. **20**(4), 375–386 (1973).

[51] P. L. Edds-Walton, "Vocalizations of minke whales Balaenoptera acutorostrata in the St. Lawrence Estuary," Bioacoustics **11**(1), 31–50 (2000).

[52] D. Risch, C. W. Clark, P. J. Dugan, M. Popescu, U. Siebert, and S. M. Van Parijs, "Minke whale acoustic behavior and multi-year seasonal and diel vocalization patterns in Massachusetts Bay, USA," Mar. Ecol. Prog. Ser. **489**, 279–295 (2013).

[53] S. Rankin and J. Barlow, "Vocalizations of the sei whale Balaenoptera borealis off the Hawaiian Islands," Bioacoustics **16**(2), 137–145 (2007).

54. S. Español-Jiménez, P. A. Bahamonde, G. Chiang, and V. Häussermann, "Discovering sounds in Patagonia: Characterizing sei whale (Balaenoptera borealis) downsweeps in the south-eastern Pacific Ocean," Ocean Sci. **15**(1), 75–82 (2019).

55. M. H. Rasmussen, J. C. Koblitz, and K. L. Laidre, "Buzzes and high-frequency clicks recorded from narwhals (Monodon monoceros) at their wintering ground," Aquat. Mamm. **41**(3), 256–264 (2015).

56. M. E. Dahlheim, "Bio-acoustics of the gray whale (*Eschrichtius robustus*)," University of British Columbia, British Columbia, Canada, 1987, https://open.library.ubc.ca/collections/ubctheses/831/items/1.0097975.

57. N. L. Crane and K. Lashkari, "Sound production of gray whales, Eschrichtius robustus, along their migration route: A new approach to signal analysis," J. Acoust. Soc. Am. **100**(3), 1878–1886 (1996).

58. R. Burnham, D. Duffus, and X. Mouy, "Gray whale (Eschrichtius robustus) call types recorded during migration off the west coast of Vancouver Island," Front. Mar. Sci. **5**, 329 (2018).

59. M. S. Soldevilla, "Risso's and Pacific white-sided dolphins in the Southern California Bight: Using echolocation clicks to study dolphin ecology", Ph.D. dissertation, University of California, San Diego, CA, 2008.

60. S. Rankin, J. Oswald, J. Barlow, and M. Lammers, "Patterned burst-pulse vocalizations of the northern right whale dolphin, Lissodelphis borealis," J. Acoust. Soc. Am. **121**(2), 1213–1218 (2007).

61. A. Alves, R. Antunes, A. Bird, P. L. Tyack, P. J. O'Malley Miller, F-P. A. Lam, and P. H. Kvadsheim, "Vocal matching of naval sonar signals by long-finned pilot whales (*Globicephala melas*)." (2014).

62. I. Foskolos, N. A. de Soto, P. T. Madsen, and M. Johnson, "Deep-diving pilot whales make cheap, but powerful, echolocation clicks with 50 μL of air," Sci. Rep. **9**(1), 15720 (2019).

63. M. H. Rasmussen and L. A. Miller, "Whistles and clicks from white-beaked dolphins, Lagenorhynchus albirostris, recorded in Faxaflói Bay, Iceland," Aquat. Mamm. **28**(1), 78–89 (2002).

64. P. Simard, D. A. Mann, and S. Gowans, "Burst-pulse sounds recorded from white-beaked dolphins (Lagenorhynchus albirostris)," Aquat. Mamm. **34**(4), 464–470 (2008).

65. A. Villadsgaard, M. Wahlberg, and J. Tougaard, "Echolocation signals of wild harbour porpoises, Phocoena phocoena," J. Exp. Biol. **210**(1), 56–64 (2007).

66. L. A. Kyhn, J. Tougaard, K. Beedholm, F. H. Jensen, E. Ashe, R. Williams, and P. T. Madsen, "Clicking in a killer whale habitat: narrow-band, high-frequency biosonar clicks of harbour porpoise (Phocoena phocoena) and Dall's porpoise (Phocoenoides dalli)," PloS One **8**(5), e63763 (2013).

67. X. Mouy, D. Hannay, M. Zykov, and B. Martin, "Tracking of Pacific walruses in the Chukchi Sea using a single hydrophone," J. Acoust. Soc. Am. **131**(2), 1349–1358 (2012).

68. G. S. Campbell, R. C. Gisiner, D. A. Helweg, and L. L. Milette, "Acoustic identification of female Steller sea lions (Eumetopias jubatus)," J. Acoust. Soc. Am. **111**(6), 2920–2928 (2002).

69. W. A. Watkins and W. E. Schevill, "Distinctive characteristics of underwater calls of the harp seal, Phoca groenlandica, during the breeding season," J. Acoust. Soc. Am. **66**(4), 983–988 (1979).

70. J. M. Jones, B. J. Thayre, E. H. Roth, M. Mahoney, I. Sia, K. Merculief, C. Jackson, C. Zeller, M. Clare, A. Bacon, S. Weaver, Z. Gentes, R. J. Small, I. Stirling, S. M. Wiggins, J. A. Hildebrand, and N. Giguere, "Ringed, bearded, and ribbon seal vocalizations north of Barrow, Alaska: Seasonal presence and relationship with sea ice," Arctic **67**, 203–222 (2014), available at https://www.jstor.org/stable/24363701.

71. K. Nikolich, H. Frouin-Mouy, and A. Acevedo-Gutiérrez, "Quantitative classification of harbor seal breeding calls in Georgia Strait, Canada," J. Acoust. Soc. Am. **140**(2), 1300–1308 (2016).

72. L. Yang, X. Xu, P. Zhang, J. Han, B. Li, and P. Berggren, "Classification of underwater vocalizations of wild spotted seals (Phoca largha) in Liaodong Bay, China," J. Acoust. Soc. Am. **141**(3), 2256–2262 (2017).

73. K. A. Ballard and K. M. Kovacs, "The acoustic repertoire of hooded seals (Cystophora cristata)," Can. J. Zool. **73**(7), 1362–1374 (1995).

74. S. McCulloch, "The vocal behaviour of the grey seal (*Halichoerus grypus*)." Ph.D. dissertation, University of St Andrews, St. Andrews, UK, 2000.

75. P. E. Nachtigall, A. Y. Supin, M. Amundin, B. Roken, T. Møller, T. A. Mooney, K. A. Taylor, and M. Yuen, "Polar bear Ursus maritimus hearing measured with auditory evoked potentials," J. Exp. Biol. **210**(7), 1116–1122 (2007).

76. L. J. McShane, J. A. Estes, M. L. Riedman, and M. M. Staedler, "Repertoire, structure, and individual variation of vocalizations in the sea otter," J. Mammal. **76**(2), 414–427 (1995).

77. S. J. Insley, "Mother–offspring vocal recognition in northern fur seals is mutual but asymmetrical," Anim. Behav. **61**(1), 129–137 (2001).

78. GEBCO Compilation Group (2019). GEBCO 2019, https://doi.org/10.5285/836f016a-33be-6ddc-e053-6c86abc0788e.

79. R. A. Locarnini, A. V. Mishonov, J. I. Antonov, T. P. Boyer, H. E. Garcia, O. K. Baranova, M. M. Zweng, and D. R. Johnson, World Ocean Atlas 2009, Volume 1: Temperature, NOAA Atlas NESDIS 68, edited by S. Levitus (U. S. Government Printing Office, Washington, DC, 2010), 184 pp.

80. J. I. Antonov, J. I., D. Seidov, T. P. Boyer, R. A. Locarnini, A. V. Mishonov, H. E. Garcia, O. K. Baranova, M. M. Zweng, and D. R. Johnson, World Ocean Atlas 2009, Volume 2: Salinity, NOAA Atlas NESDIS 69, edited by S. Levitus (U. S. Government Printing Office, Washington, DC, 2010), 184 pp.

81. P. Fleischer, W. M. Becker, and P. D. Baas, "A bottom-sediments province database and derived products, Naval Oceanographic Office," J. Acoust. Soc. Am. **130**(4), 2379 (2011).

J. Acoust. Soc. Am. **155** (1), January 2024

Heaney *et al.*   721